

Analysis of High- Accuracy Satellite Messages for Road Applications



©ISTOCKPHOTO/GREYFEBRUARY

Ignacio Fernández-Hernández

*Is with the European Commission, Brussels, Belgium.
Email: ignacio.fernandez-hernandez@ec.europa.eu*

Tommaso Senni

*Is a technical advisor for the European Commission Brussels,
Belgium. Email: t.senni@rheagroup.com*

Simón Cancela and David Calle

Are with GMV, Madrid, Spain. Email: scancela@gmv.com; jdcalle@gmv.com

Giovanni Vecchione

*Is a technical advisor for the European Commission Brussels, Belgium.
Email: g.vecchione@rheagroup.com*

Gonzalo Seco-Granados

Is with the Universitat Autònoma de Barcelona, Spain. Email: gonzalo.seco@uab.es

*Digital Object Identifier 10.1109/MITS.2020.2994074
Date of current version: 11 June 2020*

Abstract—Future road applications will require positioning accuracy on the order of one or a few decimeters and a convergence time measured in seconds. A high-accuracy service (HAS) provided by the Global Navigation Satellite System becomes a key enabler to meet these requirements. In particular, the Galileo program has committed to provide a free HAS. This entails several design challenges; namely, to achieve the necessary performance for all users, high-accuracy messages must be optimally formatted, encoded, and broadcast. This article presents an overview of satellite-based HASs and evaluates different transmission schemes based on field and laboratory results, proposing some recommendations for the implementation of an HAS. The article concludes that satellite-based, high-accuracy messages, such as Galileo’s, can provide fast convergence and sufficient accuracy worldwide, even in low-visibility environments.

Intelligent transportation systems (ITSs) are not limited to traffic congestion control and information; they also include road safety and efficient infrastructure use. One of the key enablers of ITSs is accurate and reliable vehicle location information. In the case of autonomous vehicles (AVs), the requirements for positioning performance are very stringent, and high-accuracy Global Navigation Satellite System (GNSS) solutions are a timely topic in the ITS world. GNSS receivers (Rxs) are an increasingly key element of in-vehicle systems (IVSs). Based on a recent analysis by the European GNSS Agency, IVSs could reach a 35% market penetration in the vehicle fleet in 2025 and more than 50% by 2035 [4], [2]. Fully autonomous cars will initially represent only a small fraction of the vehicles fitted with GNSS-enabled IVSs, but roughly 20% of the vehicle fleet will be autonomous by 2035. The forecast for the number of passengers and IVS-enabled and AVs is summarized in Figure 1, which shows the prospective total, in thousands, of IVSs and AVs (y -axis) between 2020 and 2035 (x -axis). (See “Acronyms Used in This Article” for explanations of the acronyms used throughout.)

AVs require decimeter-level accuracy, high availability, and integrity [3]. At the present stage, no individual technology can fulfill these requirements on its own, so sensor fusion is considered the baseline solution, with GNSS as the key sensor for absolute positioning. However, while GNSS plays a critical role in AVs, it cannot be the sole positioning source. To reach fully autonomous cars, vehicles must be able to figure out their environment, and a fusion of sensors and techniques (e.g., map matching, blind-spot monitoring, and pedestrian detection) is necessary, as shown in

Acronyms Used in This Article

API: application programming interface
 AV: autonomous vehicle
 AWGN: additive white Gaussian noise
 BEC: binary erasure channel
 CLAS: centimeter-level augmentation system
 C/N0: carrier-to-noise density ratio
 CSSR: compact state-space representation
 dBHz: decibel-hertz
 EC: error correction
 EU: European Union
 FEC: forward error correction
 FI: full interchangeability
 FR: full redundancy
 GEO: geostationary Earth orbit
 GNSS: Global Navigation Satellite System
 HAS: high-accuracy service
 ICD: interface control document
 ITS: intelligent transportation system
 IVS: in-vehicle system
 LMS: land mobile satellite
 MS: message splitting
 OS: Open Service
 PER: page error rate
 PO: page offsetting
 PPP: precise point positioning
 QZSS: Quasi-Zenith Satellite System
 RS: Reed–Solomon
 RTCM: Radio Technical Commission for Maritime
 RTK: real-time kinematic
 SBAS: satellite-based augmentation system
 SIS: signal in space
 TBC: to be confirmed
 TTRD: time to retrieve data
 URA: user range accuracy

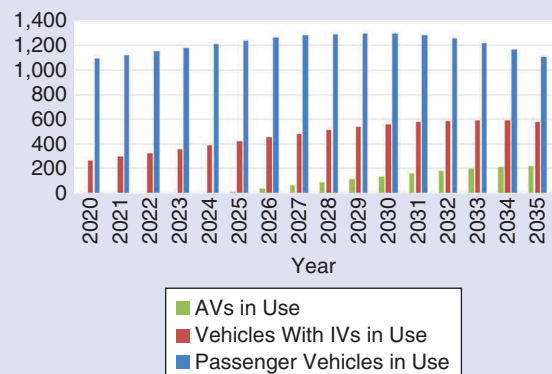


FIG 1 The global IVS-enabled and AV fleets (in thousands of units).

Figure 2. In the context of ITSs, a satellite-based HAS can bring advantages. First, an accurate GNSS-based position improves overall navigation performance and reduces the number of sensors and their cost.

Second, in some rural environments where no dedicated networks are deployed, vehicles need to rely solely on the signal in space (SIS) to obtain their position. This limitation has been highlighted in other transportation applications, such as railways, in the European Railway Traffic Management System on Satellite-Enabling Application and Validation project, which proposes GNSS signals as the main component of train location systems [4]. Finally, relying on a communications network facilitates increasing the resilience of SISs through a higher redundancy and an additional layer of security, but it also adds a potential vulnerability to hacking attacks, which may compromise other connected sensors and systems.

In addition to threats to the communication channel, jamming and, particularly, spoofing threats to a GNSS Rx need to be mitigated for robust high-accuracy positioning. The positioning device can rely on other sensors when the signal is not available due to interference. Regarding spoofing attacks, while the topic is beyond the scope of this article, solutions include signal and data authentication [5], and Galileo is implementing both in its first generation [6] as well as studying authentication of the HAS message through the SIS. These measures work well in combination with Rx-based signal processing and measurement consistency checks.

Regarding positioning integrity, it is a desirable service that could be supported by the SIS. At the moment, no integrity is foreseen for HAS SIS services beyond an indicator of the data reliability, such as user range accuracy (URA), which is already included in Radio Technical Commission for Maritime (RTCM) standards and the Quasi-Zenith Satellite System (QZSS) [8]. While the integrity of satellite-

based augmentation systems (SBASs) may support HAS services, reliability failures in the domain of ITSs may be dominated by multipath (including both line-of-sight and nonline-of-sight), and satellite malfunctions may represent only a very minor contribution. Multipath cannot be corrected by SIS data, and it may require that its computation be in the user Rx, employing Rx-autonomous integrity monitoring-like techniques and consistency checks with other sensors.

GNSS High-Accuracy and Precise Point Positioning

High-accuracy location techniques, which are understood as methods providing centimeter- or decimeter-level accuracy and are generally based on carrier phase measurements, are widely documented in the classic GNSS literature [9], [10]. They have historically been used in the domain of professional location applications, such as cadastral, construction, oil drilling, and so on. However, in recent years, there has been a commoditization of these techniques, partly because of the increasing demands of location performance from consumer users [2] and partly because of the availability of Rx's that implement such techniques at a low cost and require high-quality antennas and components that provide good carrier phase measurements, multifrequency front ends, and, potentially, ground assistance. Dual-frequency [level (L) 1–5] smartphones are already on the market, and with assistance information, they can provide accuracy on the order of decimeters [11]. Another factor that contributes to this trend is the wide availability on the Internet of high-accuracy data in real time, for example, from the International GNSS Service [12], and the open source user algorithms for precise positioning that are also available online [13]. Consumer devices, such as Google's Android, provide the GNSS measurements through a user application programming interface (API),

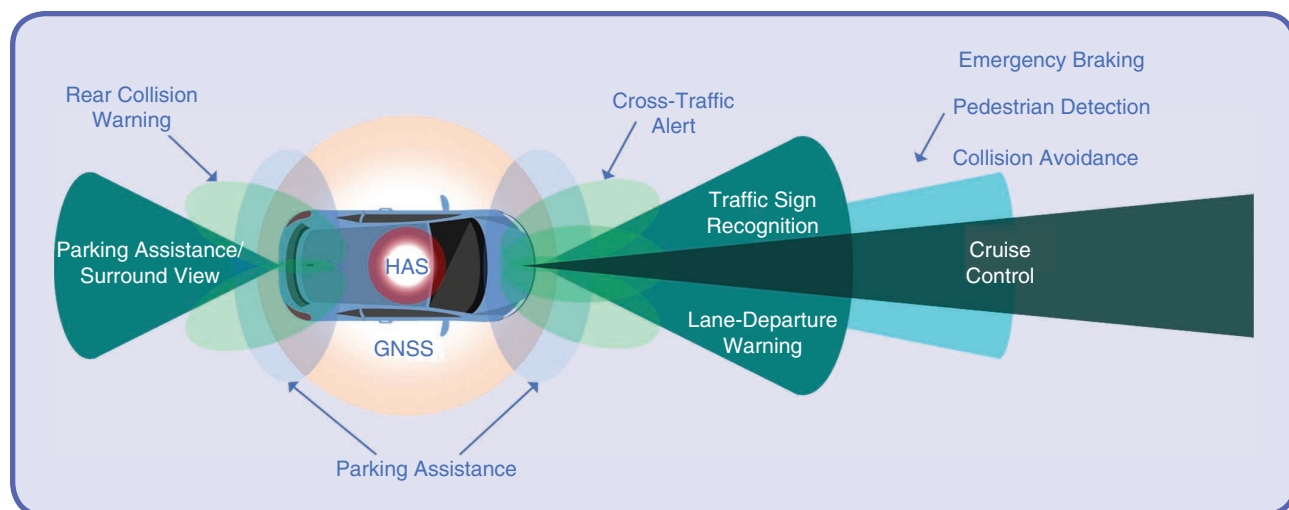


FIG 2 The GNSS high-accuracy service (HAS) in combination with other ITS sensors [7]. (The image was created by the authors based on [7].)

and they even offer tutorials explaining how to combine them into a 1-m accuracy fix [14]

On the GNSS provider side, there is a trend toward providing higher accuracy, as well: QZSS is already delivering free, high-accuracy services in Japan through the Multi-GNSS Advanced Demonstration Tool for Orbit and Clock Analysis [15] and the Centimeter-Level Augmentation System (CLAS) [8]. The Russian GNSS and the Chinese BeiDou system have also shared plans to provide high-accuracy corrections [16], [17], and Galileo, the European GNSS, has announced that it will provide a free HAS as soon as 2020 [18], with a test signal that is already available.

There are two main techniques to obtain a high-accuracy location: real-time kinematics (RTK) and precise point positioning (PPP). RTK uses differential positioning, whereby errors in the measurements of the Rx are corrected using data from a nearby station or network through the differential processing of the carrier phase measurements. On the other side, PPP uses absolute positioning techniques, whereby data and corrections for each of the original error sources (orbits, clocks, frequency biases, the ionosphere, and the troposphere, apart from local multipath and noise) are applied. The main drawback to PPP is that it may require a number of minutes to converge to a high-accuracy position, while RTK is instantaneous. The main advantage to RTK is that the technique does not require a station to be near the user.

PPP and RTK techniques are in constant evolution. A solution to improve PPP convergence is underway by using RTK techniques and a switch to PPP, a tactic called *RTK-PPP*. Another way to accelerate convergence is to provide ionospheric information to initialize the ionospheric error so that it can be more quickly decorrelated from the other error sources [19]. There are also new algorithms that take advantage of the availability of three or four frequencies that can provide an accurate fix in a matter of seconds [20]. For further details on carrier phase measurements and the RTK and PPP techniques, please consult [21, Ch. 19–23]. In the rest of this article, we focus on the transmission of high-accuracy data through GNSS signals for PPP purposes.

Satellite-Based, High-Accuracy Data Transmission

GNSS signals were originally defined to transmit data at a very low rate, such as the 50 b/s of GPS L1C/A. This low rate facilitates transmitting basic satellite information, such as ephemerides, almanacs, and a simple ionospheric model, to calculate a standard fix. However, high-accuracy data requires a greater bandwidth for reasons including multi-GNSS,

the fact that multifrequency corrections are desirable, and the need for satellite clock corrections to be refreshed very often. If all this information needs to arrive at the Rx in a short time, a higher bandwidth than the one for standard GNSS signals is required. Table 1 summarizes high-accuracy GNSS signals, including the intended coverage, number of typically available satellites, bandwidth per satellite, and band. Most satellite-based systems provide one, or at most three, links, except Galileo, which will provide four or more.

In the particular case of SBASs, rates of 250 b/s are available in both the L1 and L5 frequencies to transmit integrity, satellite corrections, and ionospheric corrections, with a submeter accuracy [22]. Commercial providers, such as Trimble/OmniSTAR, Hexagon/Veripos, and NavCom/Starfire, offer centimeter-level accuracies through GEO satellites transmitting proprietary-format messages in the L band. Further details on the data bandwidth, carrier frequencies, and accuracy services of commercial providers worldwide can be found in [23]. Some efforts have been made to reduce the bandwidth and transmit PPP corrections through lower-bandwidth channels, such as 125 b/s in an SBAS signal [24], [25] and 80 b/s in E6B [26], with remarkably good accuracy results. However, one drawback of using low bit rates for PPP is that a long time is needed to receive all the corrections. For PPP standalone applications requiring fast or instantaneous convergence, a higher bandwidth is required.

Galileo HAS

In February 2017, the European Commission formalized the addition of an HAS for Galileo [27]. At that time, the HAS was planned as a fee-based service, but one year later, the commission decided, together with European Union (EU) member states, to offer it openly and for free [18]. The main goal of providing a free HAS is to promote the public benefits of the GNSS, particularly in domains with a potentially high societal impact, such as ITSs. The current text

Table 1. Satellite signals transmitting high-accuracy data.

	Galileo	QZSS	SBAS	Commercial
Coverage	Global	Regional	Regional	Global (except high latitudes)
Satellite orbits	MEO	IGSO	GEO	GEO
Bandwidth per satellite	448 b/s	2,000 b/s	250 b/s	~2,500 b/s
Number of satellites that are typically visible (open sky)	4–6	1–3	1–2	1–2
Band/frequency	E6, 1,278.75 MHz	L6, 1,278.75 MHz	E5b, 1,207.14 MHz	L band (~1–2 GHz)

MEO: medium Earth orbit; IGSO: inclined geosynchronous orbit; GEO: geostationary Earth orbit.

explicitly mentions AVs as one of the target applications for which the HAS must be defined. The Galileo HAS message will be transmitted in the E6B signal, which modulates a Galileo message called the *commercial navigation (C/NAV) message*. Table 2 presents the main features of the E6B signal, and presents the C/NAV page structure, which includes 448 b for the HAS word.

Galileo HAS-transmitting satellites have to be connected to the ground for corrections to be uplinked, and a maximum of only 20 satellites can be linked at one time. This is due to the fact that the Galileo ground segment, at its full operational capability, includes five uplink stations with four antennas each [28]. To understand whether this poses a limitation for an HAS, Figure 3 maps the average bandwidth during a period of 10 days, a Galileo constellation of 23 nominal satellites and six spares, and a user elevation mask of 5°. This figure takes into account a realistic plan of uplink station antennas to satellites and a nominal constellation. We can see that the average bandwidth ranges between 2,704 and 3,452 b/s. The

bandwidth offered by Galileo E6B (see Table 2) is similar to other systems that offer roughly 2,000 b/s per signal for orbits and clocks. Therefore, it is sufficient for the HAS service, even after the uplink constraints. The current bandwidth should be used with an optimal coding scheme to fulfill message requirements during meager satellite availability resulting from system limitations. Optimal coding schemes will be discussed in the following sections.

Field Test Results

In 2014, the HAS feasibility using Galileo E6B was tested with a real space signal. The tests showed an accuracy of a few decimeters, even when the transmitted age of corrections was several hours [6]. Testing activities have continued, and the latest field results are presented for the first time in this article. This section presents outcomes including in-field data collection in open-sky, suburban, and urban environments, followed by postprocessing for a GPS/Galileo Rx picking up the E6B HAS message.

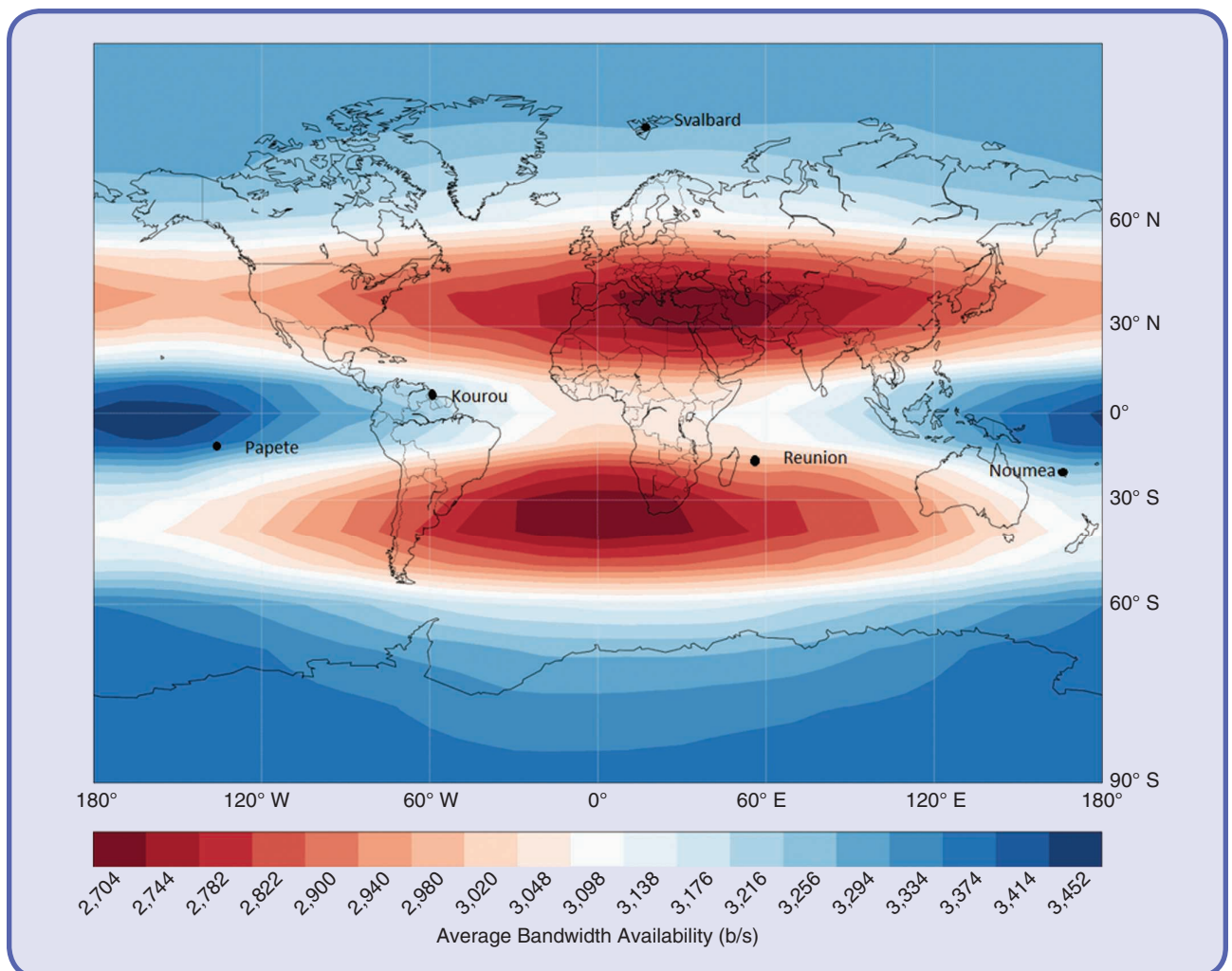


FIG 3 The average bandwidth for HAS based on a realistic 20-downlink configuration. The five uplink locations are depicted.

through urban scenarios. This is caused by environmental conditions (e.g., buildings, trees, and traffic). Figure 7 presents the horizontal accuracy obtained through the test. In the urban scenario, the accuracy is degraded, especially toward the end of the observation period, including some outliers with errors greater than 1 m when the Rx was in a traffic jam, surrounded by trucks. The RMS horizontal accuracy was fewer than 30 cm in urban environments, and fewer than 20 cm overall. The global performance was satisfactory, with some margin for performance improvements. Aspects that can enhance HAS execution for road transportation include:

- the use of more than two frequencies per GNSS, combined with trilateration techniques [20]

- the hybridization of the GNSS solution with other sensors and technologies (e.g., inertial navigation systems, odometers, and radar), as already expected for ITS applications
- the increased use of the GNSS; the selection of only high-quality, observable GNSS satellites in the PPP solution; and the integer resolution of the carrier phase ambiguities.

In any case, the test shows that satellite-based PPP can provide an accuracy of at least a few decimeters for kinematic users, even in degraded environments. However, one of the remaining problems of standard PPP is the convergence time. In the test, the first fix was obtained in approximately 30 s. However, the convergence time to a position of an error of fewer than 20 cm required more than 10 min under open-sky conditions in the static mode of operation. Figure 8 shows the results of an analysis of the convergence time of a static Rx computing a standard PPP using

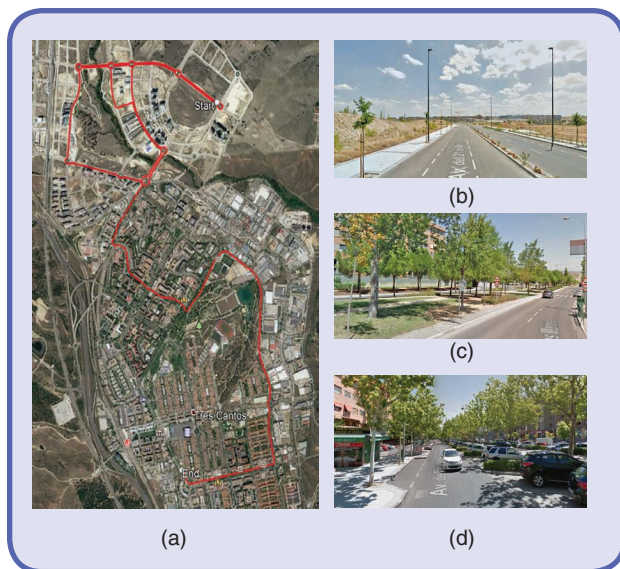


FIG 5 The trajectory for the suburban-urban HAS field scenario, which was conducted in Madrid. (a) The overview of the trajectory (imagery and maps by CNES/Google). (b)–(d) The environment types at three different places along the trajectory.

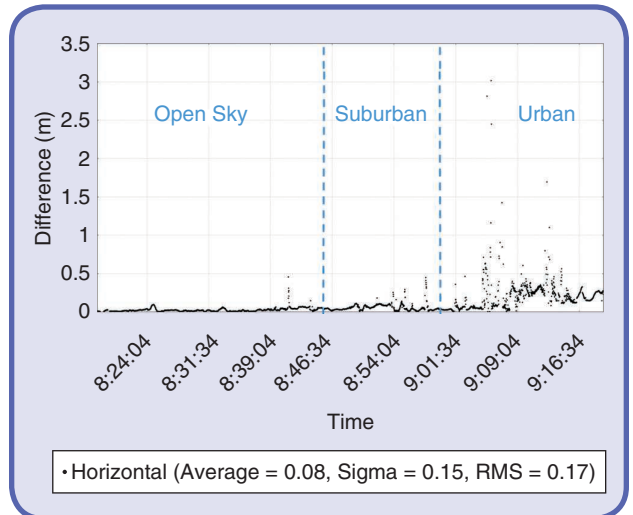


FIG 7 The horizontal accuracy of a kinematic GPS/Galileo Rx with an E6B high-accuracy message. RMS: root mean square.

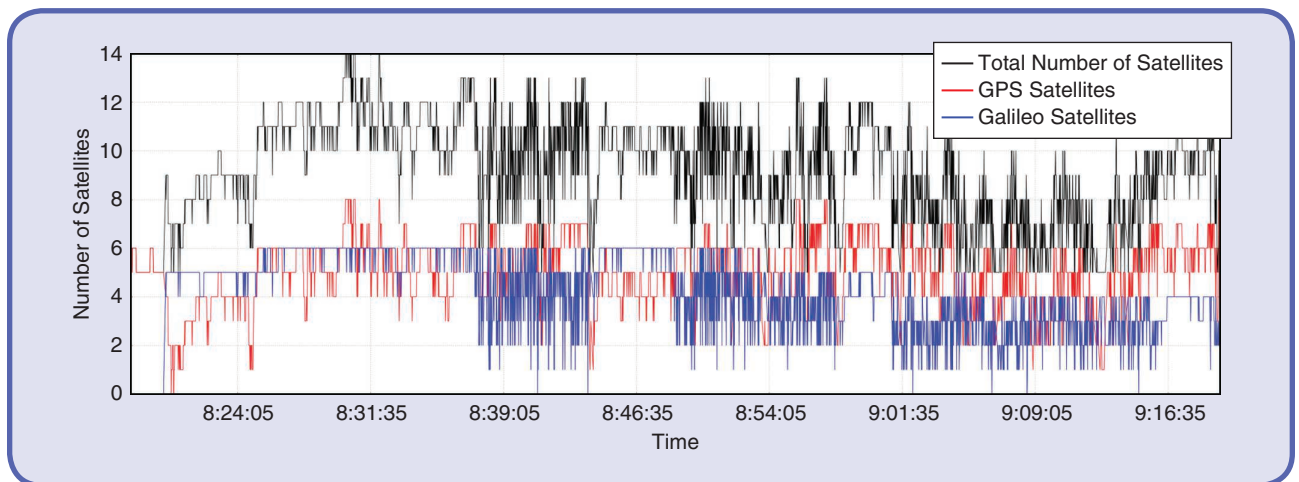


FIG 6 The number of satellites used in the PPP solution versus time, including GPS (maximum of eight), Galileo (maximum of six), and the total (maximum of 14).

only orbit and clock corrections under open-sky conditions. The values are achieved by computing 200 PPPs to derive the statistical figures for the convergences.

It is also relevant to highlight that for harsher environments (e.g., urban), which are important for automotive applications since operations usually start in these conditions, convergence times may be significantly degraded. This is especially due to the low number of satellites in view and the measurement noise, which can cause the convergence time to increase to more than 1 h with the presented configuration. These convergence times are too high for road applications, where convergence measured in seconds is sought. To improve the PPP convergence time in urban environments, more use of the GNSS, additional frequencies, and ionospheric corrections can be employed.

In addition, other vehicle and RTK-positioning sensors may be used to initialize the PPP algorithm. Considering the present and future extent of the GNSS and the number of frequencies, we can assume that near-future algorithms will provide a precise fix in a few seconds [20], including the reception of the required information. If we focus on a standalone Rx that, due to technical limitations or security constraints, calculates its fix in standalone mode, the HAS data transmission may become a bottleneck for PPP performance. In other words, an efficient satellite-based HAS message should reliably provide the necessary information as fast as possible for all potential environments so as not to delay the precise fixes.

As an illustration, Figure 9 shows several realizations and the corresponding mean of the time needed to receive the four messages (clocks and orbits for GPS/Galileo) from two Galileo satellites, *E11* and *E08*. Roughly 30 s would be necessary under open-sky conditions to receive both the orbit and the clock-correction data. In urban environments, the reception

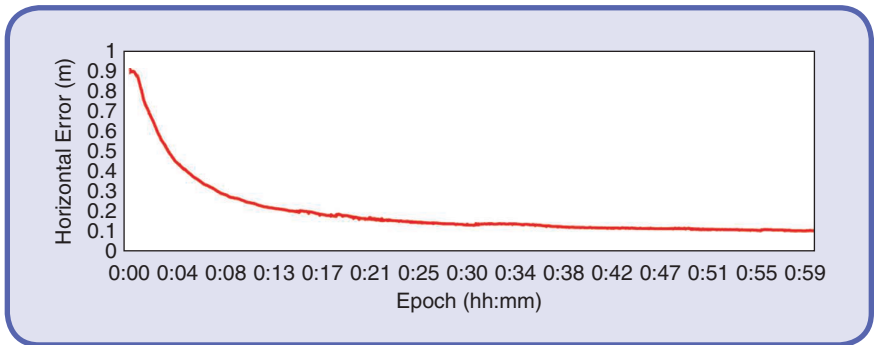


FIG 8 The PPP convergence analysis under open-sky conditions with a test configuration of two GNSS satellites, two frequencies, and no ionospheric corrections.

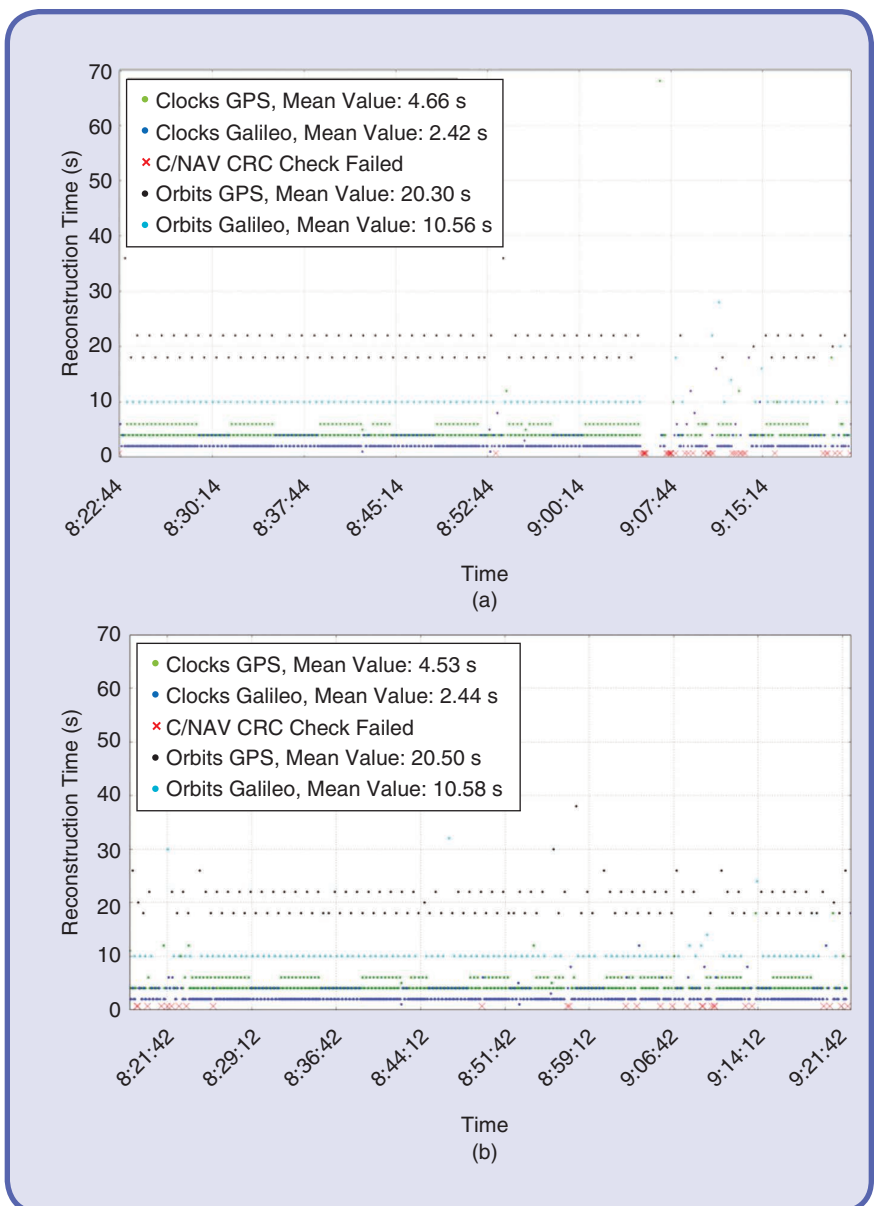


FIG 9 The reception of high-accuracy messages, orbits, and clocks for (a) *E08* and (b) *E11*. *C/NAV CRC Check Failed* shows the time elapsed since the last successful *C/NAV CRC* event.

The HAS message length may be between a few hundred and several thousand bits. The reception of a long message is challenging, given the available bit rate and 1-s page packaging, which translates into the need to receive many consecutive error-free E6B pages.

high-accuracy data are structured, packed, and encoded. At present, the Galileo HAS is expected to transmit precise orbits and clocks for Galileo and GPS, code and phase-frequency biases, and some additional signal, system, and service quality and status information. Additionally, ionospheric-correction messages may be transmitted. RTCM standards, RTCM 10403 [29] in particular, already include the required messages. A compact state-space representation

would be severely degraded. The degradation of the orbit in a few minutes does not represent a huge impact on the end-user performance in stationary mode, but it can severely affect the convergence time. The next sections study and compare several schemes to solve this problem, particularized for the Galileo system, whereby a single long message may be transmitted by several satellites.

Encoding and Transmitting an HAS Message

A main design aspect for HAS performance, in terms of both the time to retrieve the data and the accuracy, is how the

(CSSR) for RTCM [30] compresses the required information into a format that is flexible and adequate for satellite-based transmission, and it is used by the QZSS for the CLAS service [8]. The RTCM CSSR standard provides sufficient flexibility for the message update rates, number of satellites and constellations to be corrected, and correction data. The CSSR format is organized by message subtypes, enabling the dynamic allocation of orbits and clocks, code biases, and phase biases for different satellites and frequencies.

The HAS message length may be between a few hundred and several thousand bits. The reception of a long message is challenging, given the available bit rate and 1-s page packaging, which translates into the need to receive many consecutive error-free E6B pages. In addition, GNSS E6 signals coexist with amateur radio transmissions and pulse signals from radars. A qualitative analysis of HAS message packaging and coding schemes is presented as follows.

We assume a high-accuracy message M that has to be transmitted by several Galileo satellites at a given time. Full-redundancy (FR), page-offsetting (PO), message-splitting (MS), and full-interchangeability (FI) schemes are described and qualitatively compared in this section. Note that the message and block lengths are reduced with respect to realistic HAS lengths, as described in the “HAS Message Scheme Performance Comparison” section.

- **FR:** In this scheme, all satellites send the same message at the same time (Figure 10). This is the scheme used for the field test. It is represented for a four-page message ($M_1 \dots M_4$), where only the green pages are received, and the message is not obtained in the first transmission.
- **PO:** During a given interval, the same ($M_1 \dots M_4$) message is transmitted by all satellites but with a page offset. This scheme is used, e.g., for the transmission of GNSS almanacs [31] and digital signatures [32], [33]. It is illustrated in Figure 11. In this sample case, the Rx does not get the message in the first transmission, as in the previous scheme.

The next two schemes, FI and MS, require the introduction of outer-layer coding techniques to the HAS message. These two strategies are based on a message

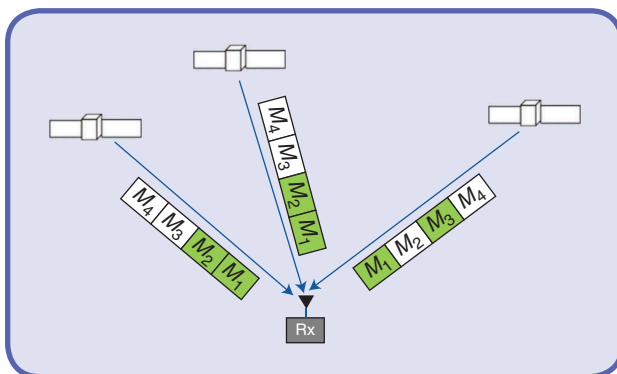


FIG 10 The FR scheme, where all satellites send the same message at the same time.

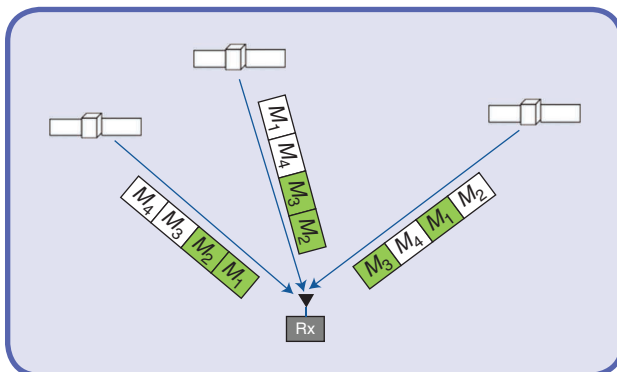


FIG 11 The PO scheme, where all satellites transmit the same message with a time offset between them.

encoded with a block-coding scheme, such as Reed–Solomon (RS) [34]. RS codes have already been proposed for the Galileo integrated navigation (I/NAV) [35]. We restate the problem as follows: Let there be a high-accuracy message M composed of k pages (M_1, \dots, M_k). The message is encoded in n pages, (C_1, \dots, C_n), $n \geq k$, and transmitted through several satellites through a binary erasure channel (BEC), which assumes that each C/NAV page (Table 3) is either received correctly or discarded. The BEC is modeled by checking the C/NAV page CRC and discarding the page if the CRC fails. Note that the outer coding layer can provide an additional error-correction capability, which will be analyzed in the “HAS Message Scheme Performance Comparison” section.

- **FI:** The message is encoded in n pages, (C_1, \dots, C_n), $n > k$, and transmitted through several satellites so that any k retrieved pages from any satellite enable the decoding of M . In this case, any page received from any satellite contributes to the message. This is illustrated in Figure 12, where we can assume that $n = 24$ and $k = 8$, and the message can be decoded since 11 packets are received. RS codes facilitate full page interchangeability, as the message can be recovered with any k symbols out of the n transmitted symbols [36]. To satisfy the FI property, n has to be much bigger than k to ensure that any encoded page received from any satellite is different from any other page during the message transmission; this is challenging because k is already high for a long message.
- **MS:** The RS decoding complexity grows exponentially with the message length. To overcome this, a long message can be split into blocks, each of which is encoded separately. However, one drawback to splitting a message is that if one block is not received, the message is incomplete. This is shown in Figure 13, where C_i^1 relates to the encoded page i of block 1 and so on. In this example, we assume the same total message length as in the FI example ($k = 8$), where four pages are encoded in each block. While the Rx gets the same number of pages, it would not get block 1 and, therefore, would not obtain the message. The purpose of this comparison is to illustrate the drawbacks of splitting a message for the sole purpose of overcoming coding restrictions.

Table 3. The C/NAV page layout.

Synchronization	Symbols			Total (Symbols)
16	984			1,000
C/NAV Page				
Reserved	HAS Page	CRC	Tail	Total (b)
14	448	24	6	492

HAS Message Scheme Performance Comparison

In this section, we compare the four previously mentioned transmission schemes for a 20-page C/NAV message. With the Galileo C/NAV 448-b page and a header of 32 b, a 20-page message could transmit 8,520 b. This is considered representative of a future HAS message because of the following:

- It is approximately the size of the GPS/Galileo orbit/clock message described for the field test (~8,070 b, according to Figure 4).
- It is also approximately the size of the GPS/Galileo 50-satellite message, including orbits, clocks, and code and phase biases for three frequencies, as shown in Table 4, according to the RTCM CSSR standard (8,082 b).
- It is also representative of an ionospheric message covering the EU area, including ~200 grid points, and enabling an interpoint distance of roughly 300 km, with 40 b per point for vertical ionospheric corrections plus headers.

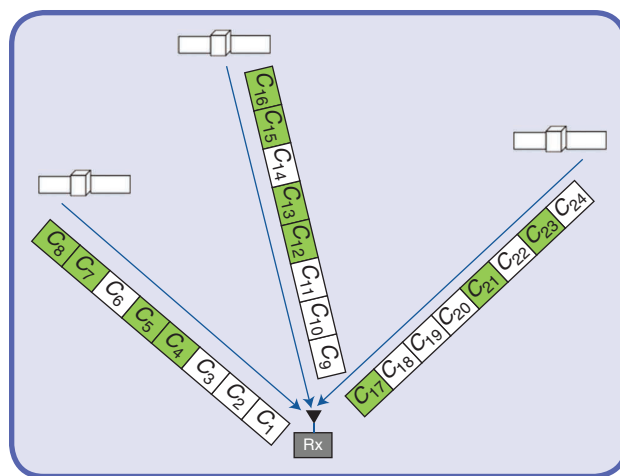


FIG 12 The FI scheme, where all pages contribute to the message decoding.

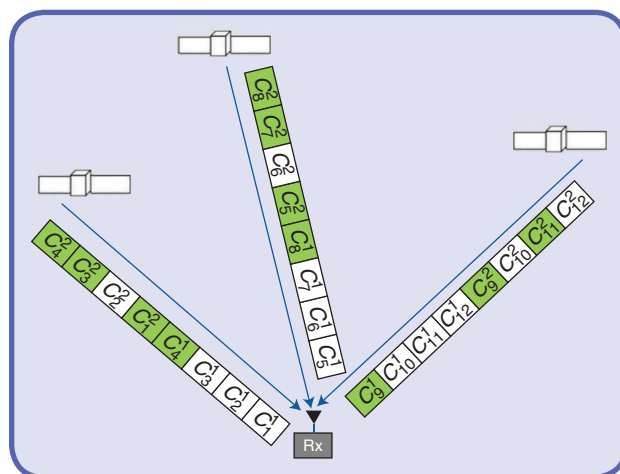


FIG 13 MS, where a long message is split into several blocks, each of which is encoded as per the FI scheme.

Our performance comparison is based on an additive white Gaussian noise (AWGN) model, a land mobile satellite (LMS) model, and a simplified BEC model. The AWGN model implements the full encoding and decoding chain for an AWGN channel at different carrier-to-noise density ratio (C/N_0) values, as described for each test. The LMS model is established on a two-state representation, as described in [37]. The simplified BEC model is founded on a MATLAB implementation of a BEC applied to a given satellite configuration, where the number of satellites and bit error rates is derived from a field test for open-sky, suburban, and urban environments. It is described in detail in [32]. In the comparison, we define a 20-page message that is continuously transmitted by all satellites. We know that a real HAS will need to interleave other messages, such as fresh clock corrections, but to relatively compare the performance of different transmission schemes, we consider this approach as the most illustrative. Table 5 summarizes the performed tests by relating the models with the transmitting schemes under evaluation. Note that the FI scheme has been tested with and without error correction (EC) in the AWGN and LMS channels.

Table 4. The message length based on CSSR subtypes 1–5 and 7 for 50 satellites ($N_{\text{sat}} = 50$), three frequencies ($N_{\text{code}} = 3$, $N_{\text{phase}} = 3$), and two GNSS satellites ($N_{\text{sys}} = 2$).

Subtype	Subtype Name	Number of Bits in Message Structure	Number of Bits
1	CSSR mask	$37 + 60 \times N_{\text{sys}}$	157
2	CSSR GNSS orbit correction	$25 + (51 \text{ or } 49) \times N_{\text{sat}}$	2,575
3	CSSR GNSS clock correction	$25 + 15 \times N_{\text{sat}}$	775
4	CSSR GNSS satellite code bias	$25 + 11 \times N_{\text{code}} \times N_{\text{sat}}$	1,675
5	CSSR GNSS satellite phase bias	$25 + 17 \times N_{\text{phase}} \times N_{\text{sat}}$	2,575
7	CSSR GNSS URA	$25 + 6 \times N_{\text{sat}}$	325
	Total bits		8,082

Table 5. The test results summary.

	AWGN	LMS	BEC
FR	X	X	X
PO	X	X	X
FI	X	X	X
FI-EC	X	X	
MS	X	X	X

AWGN Results

In this section, a performance assessment of the time to retrieve data (TTRD) is analyzed with a realistic simulator tool that was implemented in MATLAB. The tool facilitates emulating the full chain, from the transmission to the Rx, for everything that concerns the message generation, transmission, and decoding. The subframe configuration for the E6B setup includes the full E6B signal characteristics (preamble, tail, symbols rate, convolutional algorithm, and interleaving). The Rx is assumed to experience good tracking conditions to focus the comparison only on the decoding process.

The channel is configured as AWGN, with the possibility to set the C/N_0 at the desired value: good reception conditions are considered to be at 45 dBHz, while for urban environments, a value of roughly 29 dBHz is chosen. The Rx model gets the symbols out of the channel and performs the decoding into information bits, checking at the end if the decoded information is equal to the transmitted version. The output of the tool is the time needed to recover the full message. The tool is capable of multisatellite dissemination, and the Rx uses different data streams to recover the original message if one or more satellites are not visible. The number of satellites considered in the assessment is not to be understood as all satellites used for positioning; it concerns only those that are needed for retrieving the HAS corrections.

The transmission schemes implemented are FR, PO, MS, and FI. The two first cases require no extra coding layer. In the two latter cases, low-complexity, very-high-redundancy RS coding of long messages has been implemented [38], but other codes may be possible. The simulations are performed considering two visible satellites, implying that each satellite transmits a stream with a mutual offset of 10 s in the PO and MS cases, which is the best-case scenario.

AWGN: Both Satellites at 45 dBHz

The results of the simulation in open-sky conditions (45 dBHz for both satellites) are 20 s for the FR case and 10 s for the PO, MS, and FI cases, as expected, due to the lack of reception errors.

AWGN: Both Satellites at 29 dBHz

The next scenario is a situation where both satellites have a C/N_0 of 29 dBHz. The results show a considerable performance improvement thanks to the FI. At 29 dBHz, bit errors that corrupt the reception for the two configurations that rely only on the convolutional can be corrected by the RS decoding process, thus significantly improving the TTRD from between 70 and 68 s to only 14 s (95%). In this scenario, the FI enables the decoding of the message in a time period that is shorter than the message length itself (20 pages decoded after 14 s). The MS case, with

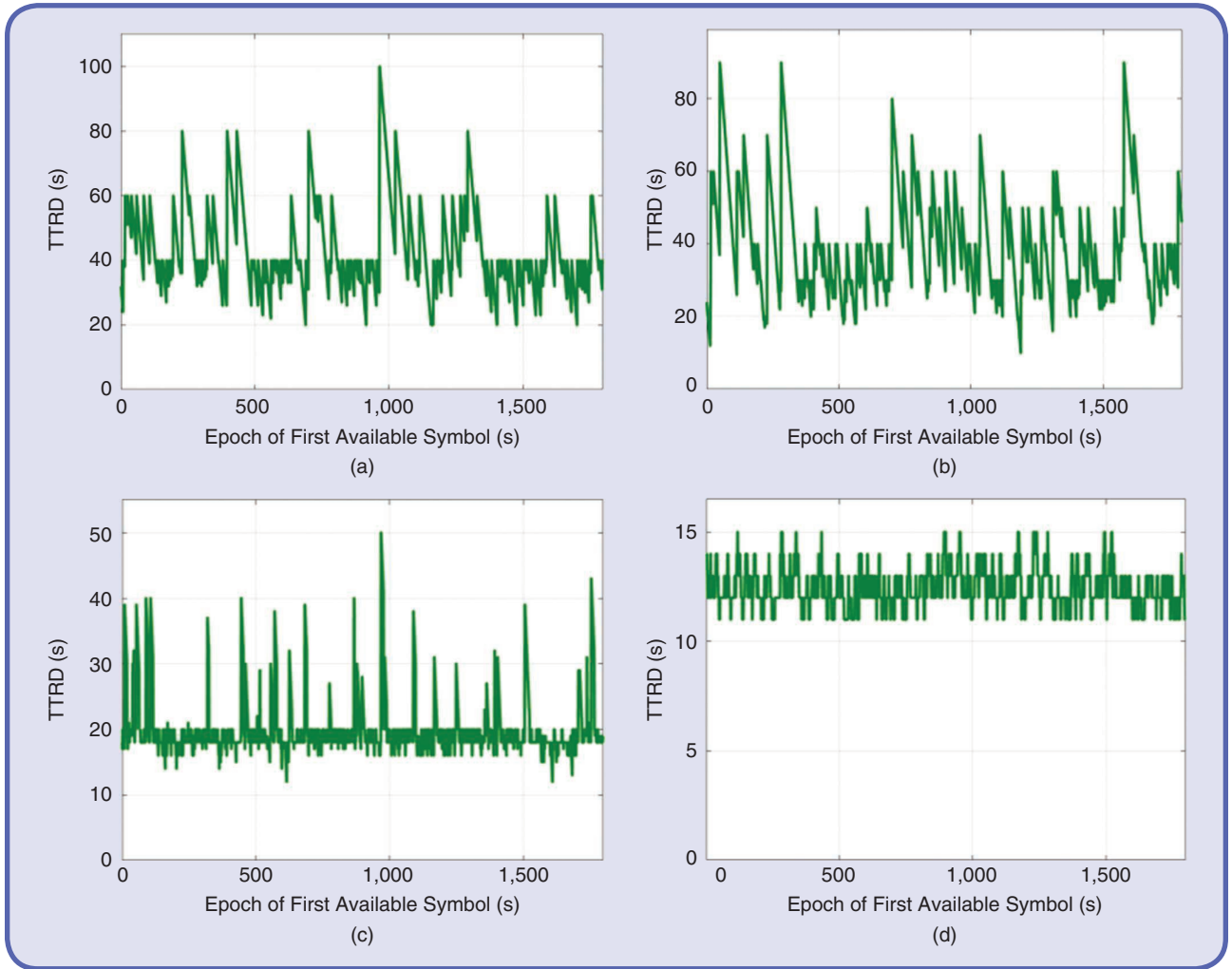


FIG 14 The reception of a 20-page message in AWGN. The (a) FR, (b) PO, (c) MS-EC, and (d) FI-EC.

its containers vertically RS encoded, offers intermediate performance between the FR and the FI. The MS-and-FI decoding case has been measured following two subcases: one in which, when the CRC is wrong, the message is discarded (MS and FC) and one in which the EC capability of the RS is used (MS-EC and FC-EC). Concerning the first case (only the pages with the correct CRC are fed into the FI algorithm), the degradation in terms of the TTRD is 7 s (95%) compared to FI-EC. Figure 14 shows the time-evolving TTRD for the four scenarios under assessment, while Table 6 presents a summary of the AWGN results.

LMS Results

In this section, the results are shown for a scenario in an LMS channel environment. The narrowband two-state channel model is used [37]. The assumptions are presented in Table 7, where two satellites are considered to be visible at a 40° elevation. While other LMS multisatellite models, such as [36], could be used, the proposed

Table 6. The FI versus the offset versus the plain 20-C/NAV-page message reception: 300/1,800-s simulation.

Two Satellites	TTRD (s): 45 dBHz		
	Average	95%	Maximum
FR	20	20	20
PO	10	10	10
MS	10	10	10
FI	10	10	10
Two Satellites	TTRD (s): 29 dBHz		
	Average	95%	Maximum
FR	43.3	70	100
PO	40	68	90
MS-EC	20.2	33	50
MS	24.1	36	49
FI-EC	12.5	14	15
FI	16.8	21	31

The Galileo HAS will be offered for free during the next few years through the Galileo E6B signal, and this article described its current status. The results of a field test including open-sky, suburban, and urban scenarios were presented, confirming that Galileo satellites will have enough bandwidth and availability to provide HASs to all users.

decoding strategies because of frequent drops in the signal power, evident in the top part (blue) of Figure 15, which leads to a high page error rate (PER). Therefore, the assumption of ideal tracking-loop conditions does not make the results less representative.

The TTRD in the time domain is shown in Figure 16 for the four scenarios under assessment in the LMS. This situation shows the advantage of the FI compared to the two configurations that have only

configuration simulates the worst-case scenario in urban environments, where the satellite coverage will be at a minimum. Using this model, two uncorrelated time series were generated for two satellites. The sample data of one satellite (satellite 1) are given in Figure 15. These series are applied to each of the two satellites during the simulations, which assume that the Rx experiences perfect tracking conditions. In other words, the phase contribution of the channel is compensated (neglected). However, the LMS channel imposes severe stress on the

the E6B convolutional code and compared to the MS. As shown in Table 8, a 25–35-s improvement (95%) is observed for the FI with respect to the FR. Table 8 also includes the results (denoted *MS* and *FI*) for the case where only the Viterbi correctly decoded pages are used in the RS decoders, and it is interesting to notice that the results are better than the ones including EC (*MS-EC* and *FI-EC*). This is similar to our findings that heavily degraded pages are disadvantageous to the RS decoding process [39]. Concerning the *MS-EC* case, (including EC), the TTRD is very similar to the FR, given that if a packet is missing within a container, the Rx needs to wait a full subframe before the same container is transmitted again. A 17-s improvement is observed for the MS with respect to the FR, but the outcome is still not as good as in the FI case, which delivers the best TTRD performance.

Table 7. The assumption for the LMS channel model.

Channel Model	Two State
Environment	Urban
Satellite elevation (°)	40
User speed (km/h)	50
Line-of-sight C/N ₀ (dBHz)	35

BEC Results

In this set of tests, three schemes are compared in a BEC channel and summarized in Table 9. In this model, the PER is randomly calculated for each page. The channel and simulation environment are further described in [37]. Based on this model, a Monte Carlo simulation is run with 10,000 instances for each scenario, measuring the time to recover the message in both cases.

The FR and FI cases are fully consistent with the ones described in previous sections. The MS scheme defined for this case deserves special mention, as it is an optimal combination of the MS (as described in the “Galileo HAS” section), PO, and FI (at the block level) evaluated in a best-case scenario. It is, therefore, named the *best-case MS plus PO*, and it is based on the following features: The message is divided into five blocks, each with four pages. Each page is encoded through a block code providing FI; i.e., every received page contributes to the block. Then, the message blocks are transmitted to each other with an offset to speed up the reception, as in the PO case. This offset is set at the best possible value for the user in each of the BEC scenarios; i.e., it provides the highest diversity to enable the quickest possible reception time. The objective of this

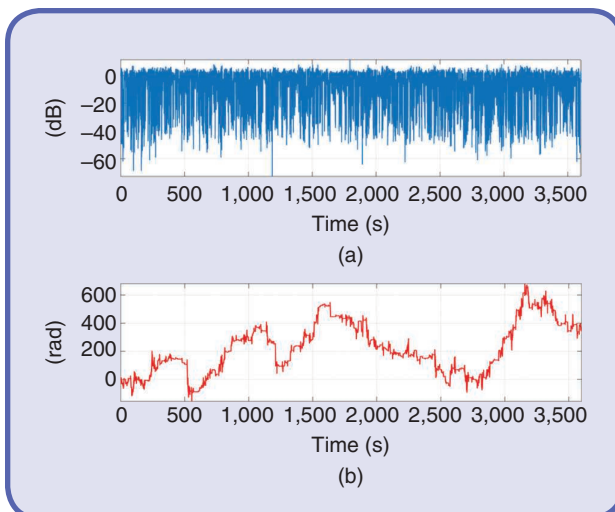


FIG 15 The LMS channel time series for satellite 1. (a) Channel attenuation. (b) Phase.

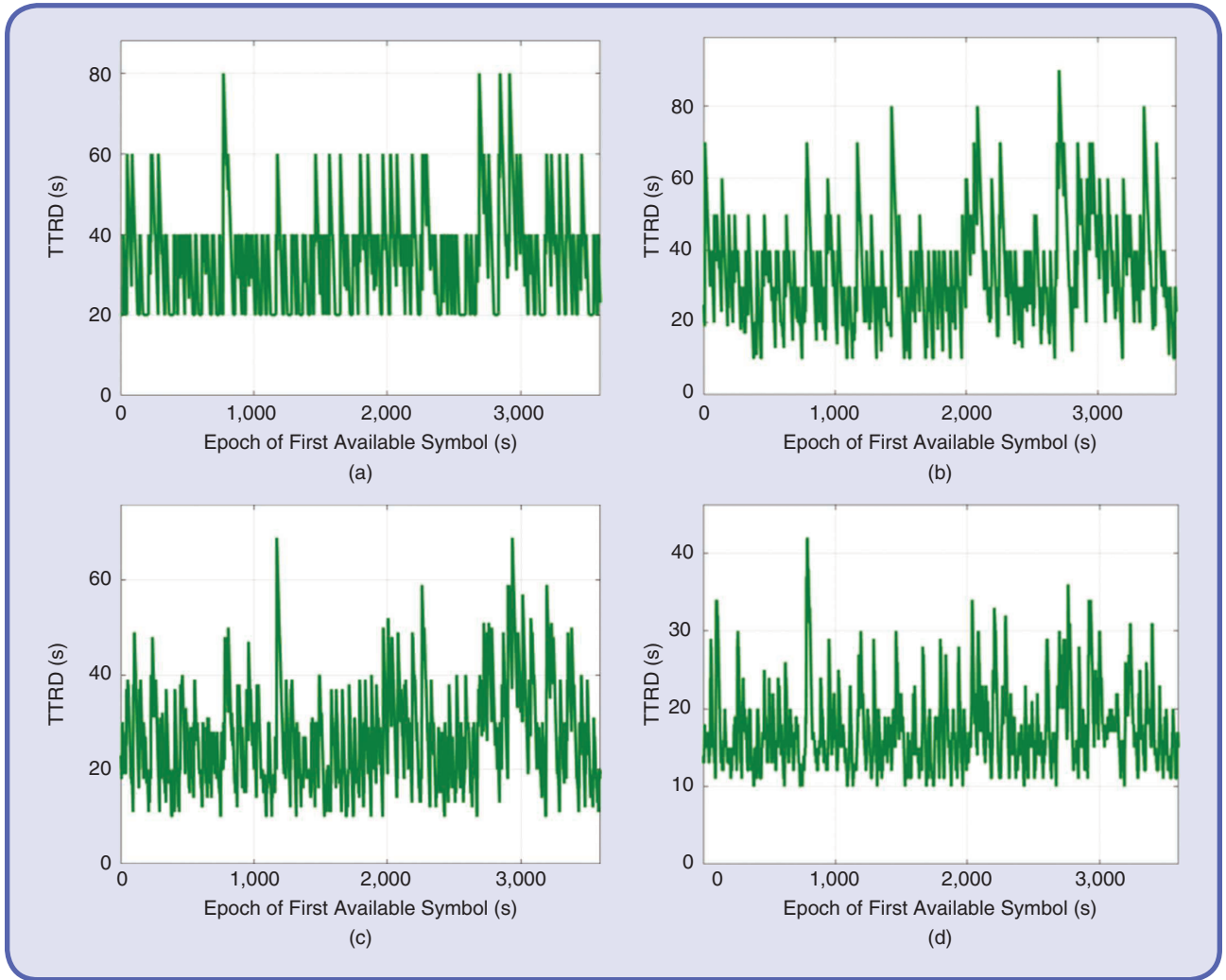


FIG 16 The reception of a 20-page message in the LMS model. The (a) FR, (b) PO, (c) MS, and (d) FI.

Table 8. The FI versus the offset versus the plain 20-C/NAV-page message reception: 3,600-s simulation.

Two Satellites	TTRD (s)		
	Average	95%	Maximum
FR	34.4	58	80
PO	34.4	62	90
MS-EC	34.1	57	82
MS	27.3	47	69
FI-EC	21.6	37	59
FI	17.5	28	42

scheme is to assess the differences between a best-case MS-PO with FI at the block level and the pure FI implementation at the message level. Because there are many alternatives for the MS and the PO, the rationale for this approach is to compare an optimal combination of the MS

Table 9. The simplified BEC description.

	Channel Model		
	Open Sky	Soft Urban	Hard Urban
SV in view	4	4	2
PER (%)	0.5 for all	1, 5, 10, and 20	10 and 20

and the PO to show that, even in this ideal case, its performance is dominated by FI.

Figure 17 conveys the results for the three transmission schemes. As expected, the FR shows the worst performance. The figure also indicates that there is a significant difference between MS and FI, as FI performs significantly better in all cases. In particular, FI enables the reception of the 20-page message in 5–7 s in open-sky and soft-urban environments (four satellites) and slightly more than 10 s in hard-urban settings (two satellites). This is also displayed

in Figure 18, which presents a histogram with the results of the three cases in the hard-urban scenario, which is the most demanding one. Note that, while the maximum bandwidth with two satellites is $448 \cdot 2 = 896$ b, the hard-urban results simulate a case in which the total average user bandwidth is 761.6 b, due to the 20% and 10% error rates on each

of the two channels ($448 \cdot 0.8 + 448 \cdot 0.9 = 761.6$). This is lower than the bandwidth in nominal system downlink conditions, as presented in Figure 3. Therefore, the results show that there is a margin to accommodate degradation in the system downlink capability while providing the HAS message at a good level of performance. The results of the tests with the BEC model are summarized in Table 10.

Conclusions

This article presented GNSS HASs for ITS and automotive applications. In particular, the article focused on cases where the vehicle cannot receive the high-accuracy message from a network and relies on a satellite-transmitted message. The Galileo HAS will be offered for free during the next few years through the Galileo E6B signal, and this article described its current status. The results of a field test including open-sky, suburban, and urban scenarios were presented, confirming that Galileo satellites will have enough bandwidth and availability to provide HASs to all users. While the accuracy can be good enough, the convergence time may be a problem for road applications. To facilitate convergence, the time to retrieve the HAS message has to be reduced. With this purpose, different message-packaging and coding schemes were proposed in this article. They are called *FR*, *PO*, *MS*, and *FI*.

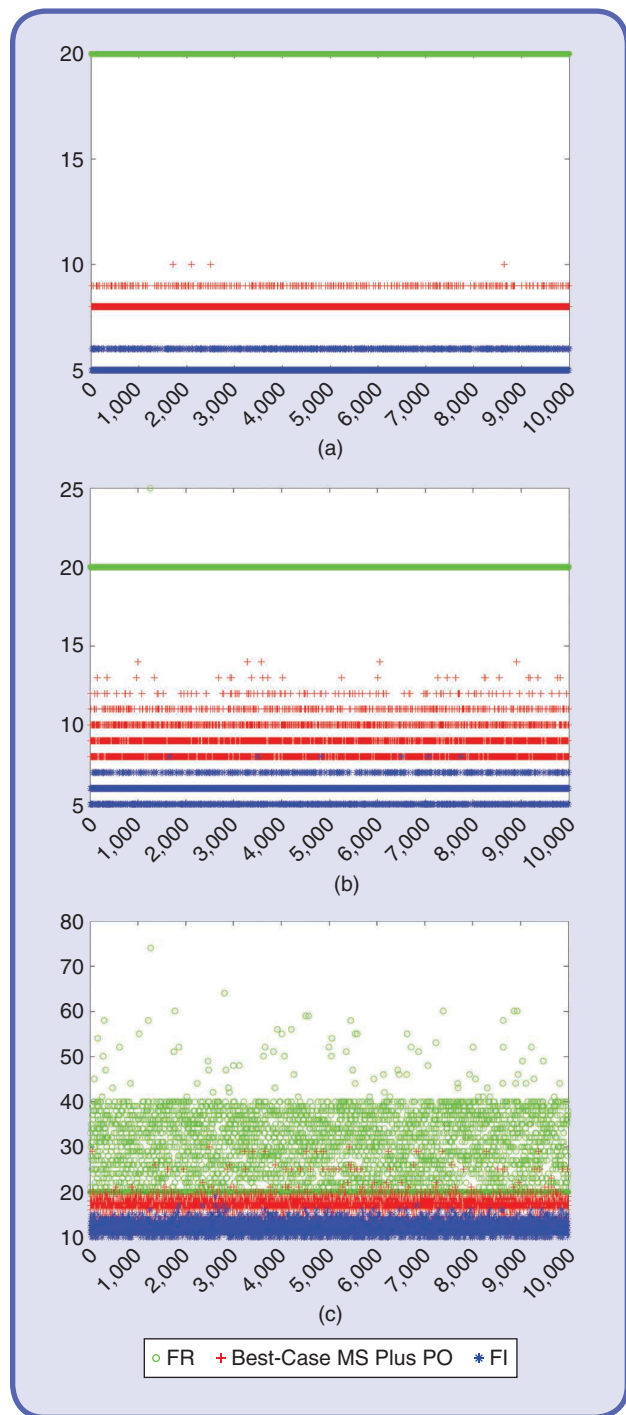


FIG 17 The reception of a 20-page message for the FR, best-case-MS-plus-PO (with FI at only block level), and FI schemes. The time for the (a) open-sky case, (b) soft-urban case, and (c) hard-urban case.

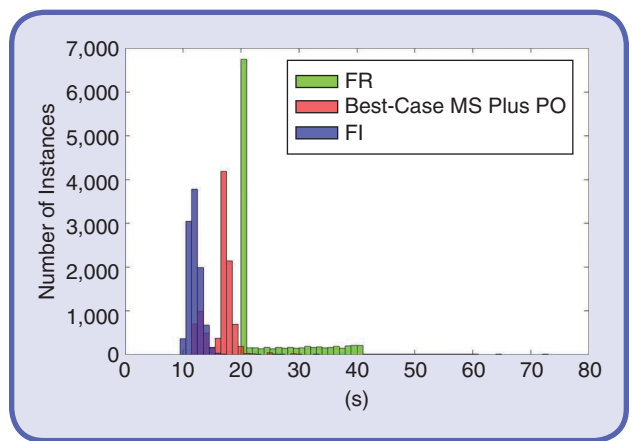


FIG 18 The HAS message reception histogram for the hard-urban, FR, best-case-MS-plus-PO, and FI cases.

Table 10. The BEC summary results for open-sky, soft-urban, and hard-urban channel modes.

	Open Sky	Soft Urban	Hard Urban
FR	Average: 20 95%: 20	Average: 20 95%: 20	Average: 23.9 95%: 38
Best-case MS plus PO	Average: 8 95%: 8	Average: 8.9 95%: 11	Average: 16.6 95%: 19
FI	Average: 5.1 95%: 6	Average: 5.9 95%: 6	Average: 12 95%: 14

The performance of the different schemes was assessed through AWGN, LMS, and BEC models, showing that the FI scheme outperforms the others. The FI scheme facilitates receiving a 20-page message ($k=20$) of 8,320 b, which is capable of providing all orbits, clocks, and three-frequency biases for any user in 6 s (open-sky and soft-urban environments) to 14 s (hard-urban conditions) with a 95% probability. These results demonstrate that an optimized coding scheme, in combination with enough measurements, sufficient frequencies, and adequate user algorithms, can contribute to almost instantaneous high-accuracy positioning, even in urban environments, at least in those locations analyzed in this article. Further work will include replacing the artificial BEC time series with field testing data for representative durations in various environments. This will enable a better understanding of how the Galileo HAS can perform when it becomes an operational service.

Acknowledgments

We would like to thank Javier Simón, Álvaro Mozo, Joaquín Reyes, and Daniel Blonski for their support during the preparation of this article and related Galileo HAS activities. The content of this article does not necessarily reflect the official position of the European Commission. Responsibility for the information and views expressed in this article lies entirely with the authors.

About the Authors



Ignacio Fernández-Hernández (ignacio.fernandez-hernandez@ec.europa.eu) earned his electronic engineering degree from ICAI, Madrid, Spain, in 2001; his M.B.A. degree from LBS, London, in 2011; and his Ph.D. degree in electronic systems from Aalborg University, Denmark, in 2015 for his research on snapshot positioning and Global Navigation Satellite System authentication. Currently, he is the Galileo Commercial Service manager at the European Commission DG GROW. In recent years, he has led the definition of authentication and high-accuracy services for Galileo. He also chairs the Galileo Commercial Service EU Working Group and the EU-US Resilience Subgroup. He has been a visiting scholar at the GPS Laboratory of Stanford University, Department of Aeronautics and Astronautics, in 2017. He is a member of the Institute of Navigation.

Currently, he is the Galileo Commercial Service manager at the European Commission DG GROW. In recent years, he has led the definition of authentication and high-accuracy services for Galileo. He also chairs the Galileo Commercial Service EU Working Group and the EU-US Resilience Subgroup. He has been a visiting scholar at the GPS Laboratory of Stanford University, Department of Aeronautics and Astronautics, in 2017. He is a member of the Institute of Navigation.



Tommaso Senni (t.senni@rheagroup.com) earned his B.Sc. degree in electronic engineering from Perugia University and his M.Sc. degree in telecommunication engineering from Università degli Studi di Roma. Currently, he is the EGNSS signal advisor at the European

Commission DG GROW, where he works on the definition of Galileo first generation and second generation services. He is a system engineer specializing in satellite navigation systems with experience in GNSS systems, GNSS applications, and signal processing. He has been a SIS engineer at the ESA/ESTEC and a system engineer at IFEN GmbH and Space Engineering, S.p.a.



Simón Cancela (scancela@gmv.com) earned his M.Sc. degree in advanced mathematics from the Universidad Complutense de Madrid, Spain. He joined GMV in 2015, and he has been working in the Galileo Commercial Service Demonstrator validation and experimentation activities. Currently, he is working on the development of a Commercial Service-enhanced PVT-resilient platform.



David Calle (jdcalle@gmv.com) earned his M.Sc. degree in computer engineering from the University of Salamanca. He joined GMV in 2008, and he has been working in the GNSS business unit involved in the design and development of GNSS algorithms, applications, and systems. He is currently head of the GNSS Advance Services Section, coordinating the activities related to the Galileo Commercial Service, Open Service Authentication, and High-Accuracy provision services.



Giovanni Vecchione (g.vecchione@rheagroup.com) earned his M.Sc. degree in telecommunications engineering with a master in navigation and related applications from Politecnico di Torino and ISMB (Istituto Superiore Mario Boella). He is a senior telecommunication engineer working as a Galileo commercial service adviser for the European Commission DG GROW. In the last year, he has been involved in the definition of high accuracy service and OSNMA for the first Generation of Galileo, the European Satellite Navigation program.



Gonzalo Seco-Granados (gonzalo.seco@uab.es) earned his Ph.D. degree in telecommunications engineering from the Universitat Politècnica de Catalunya, Spain, in 2000 and his M.B.A. degree from the IESE Business School, Barcelona, Spain, in 2002. He is currently a professor in the Department of Telecommunication,

Universitat Autònoma de Barcelona, where he has served as the vice dean of the Engineering School during 2011–2019. From 2002 to 2005, he was a member of the European Space Agency, where he was involved in the design of the Galileo System. In 2015 and 2019, he was a Fulbright Visiting Researcher at the University of California, Irvine. Since 2018, he has been serving as a member of the Sensor Array and Multichannel Technical Committee for the IEEE Signal Processing Society. Since 2019, he has been the president of the Spanish Chapter of the IEEE Aerospace and Electronic Systems Society. He has received the ICREA Academia Award in 2015 and 2019. His research interests include satellite and terrestrial localization systems. He is a Senior Member of the IEEE.

References

- [1] T. Litman, "Autonomous vehicle implementation predictions, implications for transport planning," Victoria Transport Policy Inst., Victoria, BC, 8 Sept. 2017.
- [2] "G2019 GSA GNSS Market Report," no. 6. European Global Navigation Satellite Systems Agency, Prague, Czech Republic, Oct. 15, 2019. [Online]. Available: https://www.gsa.europa.eu/system/files/reports/market_report_issue_6_v2.pdf
- [3] "SaPPART white paper: Satellite positioning performance assessment for road transport," IFSTTAR, Marne la Vallée, France, White Paper, 2015. [Online]. Available: <https://www.rapp.ch/en/references/satellite-positioning-performance-assessment-road-transport-sappart>
- [4] ERSAT—EAV. "ERTMS on SATELLITE—Enabling application & validation," ERSAT EAV Consortium, 2016. Accessed on: Dec. 2019. [Online]. Available: <http://www.ersat-eav.eu/>
- [5] D. Magaria, B. Motella, M. Anghileri, J. J. Floch, I. Fernández-Hernández, and M. Paonni, "Signal structure-based authentication for civil GNSSs: Recent solutions and perspectives," *IEEE Signal Process. Mag.*, vol. 34, no. 5, pp. 27–37, 2017. doi: 10.1109/MSP.2017.2715898.
- [6] I. Fernández-Hernández et al., "Testing GNSS high accuracy and authentication: Galileo's commercial service," *Inside GNSS*, pp. 37–48, Jan.–Feb. 2015.
- [7] "Inside GNSS webinar safety critical positioning for automotive," *Inside GNSS*, 2016. [Online]. Available: <https://insidegnss.com/download/inside-gnss-webinar-safety-critical-positioning-for-automotive-video/>
- [8] "Quasi-Zenith satellite system interface specification centimeter-level augmentation service," Cabinet Office, Tokyo, Rep. no. IS-QZSS-L6-001, draft edition, 2017. Available: <https://qzss.go.jp/en/technical/download/pdf/ps-is-qzss/is-qzss-l6-001.pdf>
- [9] P. Misra and P. Enge, *Global Positioning System: Signals, Measurements and Performance*, Lincoln, MA: Ganga-Jamuna Press, 2011.
- [10] B. Hofmann-Wellenhof, H. Lichtenegger, and E. Wasle, *GNSS- Global Navigation Satellite Systems: GPS, GLONASS, Galileo, and more*, New York: Springer-Verlag, 2008.
- [11] "World's first dual-frequency GNSS smartphone hits the market," European Global Navigation Satellite Systems Agency, Prague, Czechia, 4 June 2018. Accessed on: Sept. 2018. [Online]. Available: <https://www.gsa.europa.eu/newsroom/news/world-s-first-dual-frequency-gnss-smartphone-hits-market>
- [12] "Real-time service," International GNSS Service, Dublin, OH. Accessed on: Sept 2018. [Online]. Available: <http://www.igs.org/rts/products>
- [13] "RTKLIB: An open source program package for GNSS positioning." Accessed on: Sept 2018. [Online]. Available: <http://www.rtklib.com/>
- [14] F. van Diggelen, R. Want, and W. Wang, "How to achieve 1-meter accuracy in Android," *GPS World*, 5 July 2018. [Online]. Available: <https://www.gpsworld.com/how-to-achieve-1-meter-accuracy-in-android/>
- [15] *Interface Specification for MADOCA-SEAD*, Japan Aerospace Exploration Agency, Tokyo, Feb. 2017. [Online]. Available: https://ssl.tksc.jaxa.jp/madoca/public/doc/Interface_Specification_A_en.pdf
- [16] S. Goff, "China plans to launch two BeiDou-2 backup satellites in the next 2 years," *Inside GNSS*, May 31, 2018. [Online]. Available: <https://insidegnss.com/china-plans-to-launch-two-beidou-2-backup-satellites-in-the-next-2-years/>
- [17] P. G. Stupak, "SDCM present status and future: GLONASS signals development," presented at the Proc. 8th Meeting Int. Committee Global Navigation Satellite Systems, Nov.9–14, 2015, Dubai. [Online]. Available: http://www.unoosa.org/pdf/icg/2015/icg-8/wgA/A1_2.pdf
- [18] European Commission, "Commission Implementing Decision (EU) 2018/521 of 2 March 2018 Amending Implementing Decision (EU) 2017/224 (CS Implementing Act)," Mar. 2, 2018. [Online]. Available: https://eur-lex.europa.eu/eli/dec_impl/2018/521/oj
- [19] A. Rovira-García, J. Juan, J. Sanz, G. González-Casado, and E. Bertran, "Fast precise point positioning: A system to provide corrections for single and multi-frequency navigation," *Navigation, J. Inst. Navigation*, vol. 65, no. 3, pp. 251–247, 2016. doi: 10.1002/navi.148.
- [20] D. Laurichesse and S. Banville, "Instantaneous centimeter-level multi-frequency precise point positioning," *GPS World J.*, vol. 29, no. 4, July 2018.
- [21] P. J. Teunissen and O. Montenbruck, *Springer Handbook of Global Navigation Satellite Systems*. New York: Springer-Verlag, 2017.
- [22] *Minimum Operational Performance Standards for Global Positioning System: Wide Area Augmentation System Airborne Equipment: DO229E*, RTCA SC-159, Dec. 15, 2016.
- [23] S. Choy, J. Kuckartz, A. G. Dempster, C. Rizo, and M. Higgins, "GNSS satellite-based augmentation systems for Australia," *GPS Solutions*, vol. 21, no. 3, pp. 855–848, 2017. doi: 10.1007/s10291-016-0569-2.
- [24] M. Abault-Roudier et al., "A demonstration of the Galileo E5b signal," *Inside GNSS*, Jan./Feb. 2018. [Online]. Available: <https://insidegnss.com/wp-content/uploads/2018/04/janfeb18-WP.pdf>
- [25] J. Barrios et al., "Update on Australia and New Zealand DFMC SBAS and PPP system results," in *Proc. Int. Tech. Meeting Satellite Division Institute of Navigation (ION GNSS+ 2018)*, Miami, FL, 2018, pp. 1058–1067.
- [26] D. Calle, S. Cancela, E. Carbonell, I. Rodríguez, G. Tobías, and I. Fernández-Hernández, "First experimentation results with the full Galileo CS demonstrator," in *Proc. Int. Tech. Meeting Satellite Division Institute of Navigation (ION GNSS+ 2016)*, Portland, OR, 2016, pp. 2870–2877. doi: 10.55012/2016.14728.
- [27] European Commission, "Commission Implementing Decision (EU) 2017/224 of 8 February 2017 (CS Implementing Act)," 2017. [Online]. Available: <https://eur-lex.europa.eu/legal-content/EN/TXT/?uri=CELEX%3A52017D0224>
- [28] J. Pérez-Bartolomé, X. Maufroid, I. Fernández-Hernández, J. A. López-Salcedo, and G. Seco-Granados, "Overview of Galileo system," in *Galileo Positioning Technologies*, J. Nurmi, E. Lohan, S. Sand, and H. Hurkainen, Eds. New York: Springer-Verlag, 2015, pp. 9–35.
- [29] *RTCM Standard 1040.2: Differential GNSS Service—Version 3—SC 104*, RTCM SC 104, 2013.
- [30] R. Hirokawa, Y. F. S. Sato, and M. Miya, "Compact SSR messages with integrity information for satellite based PPP-RTK service," in *Proc. Int. Tech. Meeting Satellite Division Institute of Navigation (ION GNSS+ 2016)*, Portland, OR, 2016, pp. 3572–3576. doi: 10.55012/2016.14794.
- [31] European Union, "OSSISICD: Open service signal in space interface control document, Issue 1.5," 2016. [Online]. Available: <https://www.gsc-europa.eu/sites/default/files/sites/all/files/Galileo-OS-SIS-ICD.pdf>
- [32] I. Fernández-Hernández, J. D. C. Calle, S. Cancela, O. Pozzobon, C. Sarto, and J. Simón, "Packet transmission through navigation satellites: A preliminary analysis using Monte Carlo simulations," in *Proc. European Navigation Conf., (ENC 2017)*, Lausanne, CH, 2017, pp. 298–304.
- [33] I. Fernández et al., "Fountain Codes for GNSS," in *Proc. Int. Tech. Meeting Satellite Division Institute of Navigation (ION GNSS 2017)*, Portland, OR, 2017, pp. 1496–1507.
- [34] I. S. Reed and G. Solomon, "Polynomial codes over certain finite fields," *J. Soc. Ind. Appl. Math.*, vol. 8, no. 2, pp. 300–304, 1960. doi: 10.1157/0108018.
- [35] B. E. Schotsch, M. Anghileri, M. Ouedraogo, and T. Burger, "Joint time-to-CED reduction and improvement of CED robustness in the Galileo I/NAV message," in *Proc. 30th Int. Tech. Meeting Satellite Division Institute of Navigation (ION GNSS+ 2017)*, Portland, OR, 2017, pp. 1544–1558.
- [36] J. Westall and J. Martin, "An introduction to Galois fields and Reed-Solomon coding," School of Computing Clemson Univ. Clemson, SC, Oct. 4, 2010. [Online]. Available: <https://people.cs.clemson.edu/~westall/851/rs-code.pdf>
- [37] A. Jahn, H. Bischl and G. Heib, "Channel characterisation for spread spectrum satellite communication," in *Proc. IEEE 4th Int. Symp. Spread Spectrum Techniques and Applications*, 1996, pp. 1221–1226. doi: 10.1109/ISSSTA.1996.563500.
- [38] I. Fernández-Hernández, "Method and system for optimized satellite navigation message transmission," EU Patent 18 199 280, Oct. 2018.
- [39] D. Borio, M. Susi, T. Senni, and I. Fernández-Hernández, "The Galileo E6-B propagation channel: An experimental characterization," in *Proc. Ka and Broadband Communications Conf.*, Sorrento, IT, 2019, pp. 1–8.